

Contiguous-Domain Transferred-Electron Oscillators

James A. Cooper, Jr.
 School of Electrical Engineering
 Purdue University
 West Lafayette, IN 47907

K. K. Thornber
 AT&T Bell Laboratories
 Whippany, NJ 07981

SUMMARY

We describe a new monolithic millimeter-wave semiconductor oscillator which is capable of supporting a *contiguous sequence* of charge domains in the drift channel. The frequency is not determined by a transit time effect, but rather by the spacing between adjacent domains, and can be electrically tuned from a few gigahertz to a few hundred gigahertz.

INTRODUCTION

We describe a new type of monolithic millimeter-wave semiconductor oscillator called a contiguous-domain transferred-electron oscillator.¹ This new device makes a clean break from the operating principles of existing devices, and thereby escapes many of their fundamental limitations.

"Conventional" microwave semiconductor oscillators include both the transferred-electron (Gunn effect) devices and the IMPATT, BARITT, TRAPATT, and other related transit-time devices. In spite of their diversity, all these devices share four common characteristics which limit their performance:

- (1) They normally operate as negative conductance circuit elements into an external tuned circuit or resonant cavity. Tuning can only be accomplished by changing the resonant frequency of the external circuit.
- (2) They have only two terminals, so that the internal electrostatics are inherently one-dimensional and are closely coupled to the voltage excursions in the external circuit.
- (3) Their operation consists of the transient formation, propagation, and dispersal of pulses of charge.
- (4) They are capable of supporting at most only one charge packet at a time in the drift channel.

As a result of these common characteristics, all existing devices are limited in frequency by the transient response times of their carrier distributions and by the transit time of charge packets across their drift regions. Advancements in semiconductor oscillators have been achieved primarily by reducing the length of the drift regions to sub-micron dimensions. It is clear that fundamental physical limits are at hand, and that new device concepts are needed.

The contiguous-domain device differs from all preceding semiconductor oscillators in that *none* of these four limiting characteristics apply. In particular, our device does *not* require an external resonant circuit, does *not*

rely on the transient formation, drift, and dispersal of pulses of charge, and is capable of creating and supporting a *contiguous sequence* of charge domains within the drift channel. As a result, the frequency is not determined by a transit-time effect, but rather by the spatial period of the sequence of charge domains drifting down the channel in steady state. Thus, there is no need for sub-micron dimensions in order to achieve high frequency. Moreover, since there is no external resonant circuit, the frequency can be tuned over a broad band simply by controlling the rate at which charge is introduced into the drift channel. Calculations indicate that the frequency can be tuned from a few gigahertz to a few hundred gigahertz in a time as short as a few periods of the oscillation frequency itself. The device structure is compatible with existing GaAs planar integrated circuit technology, both MESFET and MODFET, so that direct integration with active signal processing elements should be straightforward.

DEVICE DESCRIPTION

In order to allow a contiguous sequence of charge domains to coexist in the drift channel, it is necessary to modify the electrostatic boundary conditions so that the local fields of each domain are screened from the rest of the channel. We can accomplish this using the device structure shown in Fig.1. This structure is similar to that of a GaAs MESFET except that the gate is formed by a resistive thin film and contacts are established at each end. A potential drop is applied between G1 and G2 so that a uniform electric field exists along the gate. The drain is biased positive with respect to G2 and the source slightly positive with respect to G1. Under these conditions, a potential barrier will exist in the buried channel under the source end of the gate, preventing electrons from entering the channel from the source. Since the drain is the most positive terminal in the device, any electrons in the channel will be drawn down the channel and into the drain, leaving the channel totally depleted. The energy band diagram for this situation is shown in Fig.2.

The potential ϕ_m at the channel minimum (in the absence of electrons in the channel) can be written²

$$\phi_m = V_g - V_B + qN_d d^2 / 2\epsilon_s \quad (1)$$

where V_g is the gate voltage (a function of position) V_B the metal-semiconductor barrier height, q the electronic charge, N_d the epitaxial layer doping, d the thickness of the epi layer, and ϵ_s the semiconductor permittivity. Clearly, ϕ_m is equal to V_g within a constant value. Since the gate potential varies linearly along the channel, the potential of the bottom of the potential well in the channel also varies linearly with position, and the x-

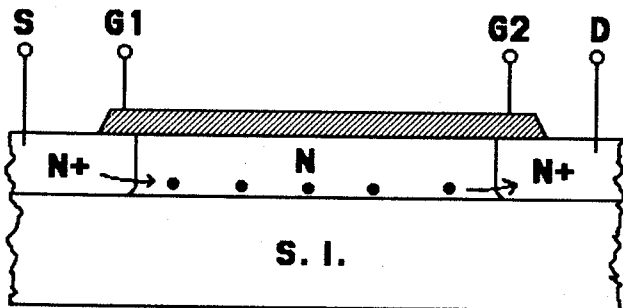


Figure 1. The MESFET-like version of the oscillator. The resistive gate forms a Schottky barrier to the channel, which is depleted except for electrons injected from the source. These electrons are confined to the potential minimum near the bottom interface, and rearrange in response to the lateral electric field impressed by the resistive gate. Also shown is a schematic plot of the potential at the channel minimum versus distance.

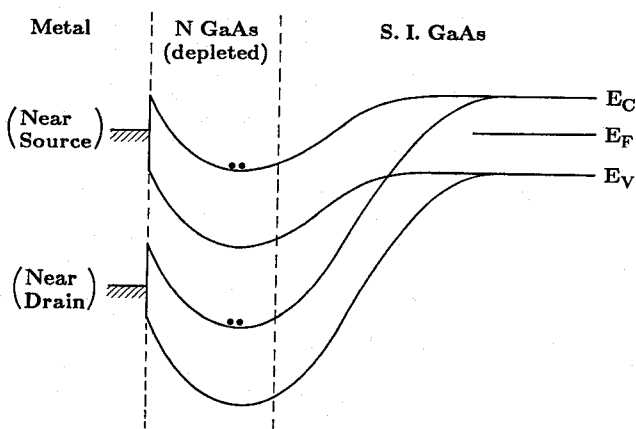


Figure 2. Band diagrams perpendicular to the surface of the device in Fig. 1. The n-type GaAs layer is depleted of electrons (except for those shown), so that a deep potential minimum exists near the bottom interface. As the gate voltage becomes more positive (moving toward the drain), E_F in the metal moves down, and the minimum deepens linearly with position, resulting in a uniform field moving electrons toward the drain.

component of the electric field is uniform at V_{gg}/L , where V_{gg} is the voltage across the resistive gate, and L is the gate length. If electrons are now introduced into the channel (by reducing the potential of the source), they will enter a region of constant electric field and drift down the channel into the drain. If the electric field imposed by the gate is in the regime of negative differential mobility for electrons in GaAs, any small fluctuations in the electron density will grow (as in a Gunn diode), and domains will form. However, since the field in the channel is established by the linear potential variation of the gate (and *not* by the electrodes at the ends of the drift region, as in conventional two-terminal devices), the image charges of the domains *must* reside on the nearby gate. As a result, the gate effectively screens the remainder of the drift channel from the local self-induced fields of each domain, and a contiguous sequence of domains can be supported all along the channel, since the field remains in the regime of negative differential mobility all along the channel. The frequency of the oscillations in the drain circuit is then determined by the spatial period of the sequence of contiguous domains in the channel and by the drift velocity.

We note in passing that one can create the same type of electrostatic boundary conditions by using a MODFET (or HEMT) structure, and confining electrons in the potential well at the GaAs/AlGaAs interface. All of the preceding arguments about device operation go through in an analogous fashion.

ANALYSIS

In order to predict the period and amplitude of the domains in the channel of these devices, we have performed both computer and analytical calculations. The analytical theory will be presented elsewhere. Here, we will discuss the computer program and show some of the results of the computer analysis.

The computer program performs a transient analysis of the buildup and drift of charge fluctuations in the channel of the device. It is based on one-dimensional electrostatics, and operates in the following manner: First, the channel is divided into a uniform grid from source to drain. We know the gate potential at each grid point, and we assume some initial charge density per unit area in the channel at each grid point. Knowing these items, we calculate the potential at the channel minimum at each grid point using one-dimensional electrostatics. (Actually, the potential is corrected by a Green's function perturbation term³ which includes the influence of charges in nearby grids. By adding this correction term, we are effectively eliminating the gradual channel approximation.) Knowing the potential, we calculate the electric field acting between grid points. We then determine the carrier drift velocity and diffusion coefficient at each grid point from empirical equations based on measured data. From the charge density, drift velocity, and diffusion coefficient at each grid point, we calculate the carrier flux. Multiplying this flux by a small time increment Δt and applying the continuity equation gives the new charge density at each grid point at the next time step. Care was taken that the spatial and temporal grid sizes were small enough that the results did not vary with changes in either grid size.

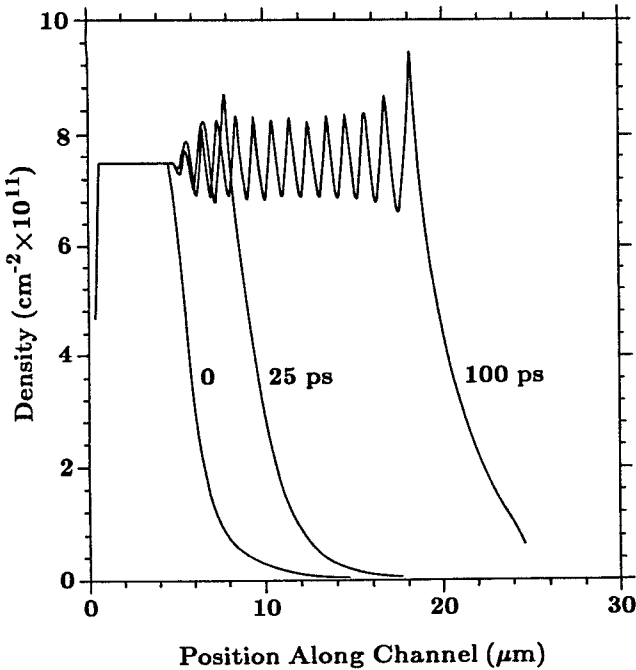


Figure 3. The time evolution of electron density in the channel as electrons are introduced from the source. Here, the source is modeled by holding the electron density constant at $\bar{n} = 7.5 \times 10^{11} \text{ cm}^{-2}$ from $x=0$ to $x=5 \mu\text{m}$. In this simulation (which was actually run for the MODFET version of the device), $\mathbf{d} = 500 \text{ \AA}$ and the drift field is 7000 V/cm.

An illustration of the transient build-up and drift of domains in the channel is shown in Fig. 3. Here we have introduced electrons into the channel at the source ($x=20 \mu\text{m}$), beginning at $t=0$. (The electron concentration per unit area is fixed at $7.5 \times 10^{11} \text{ cm}^{-2}$ for all $x \leq 20 \mu\text{m}$.) As electrons enter the channel from the source, spatial oscillations form spontaneously. Behind the moving charge front, the oscillations quickly stabilize, assuming a uniform amplitude and period. These stable oscillations in the electron density may be regarded as domains, since the electron distribution is now in steady state with respect to the drifting reference frame. Once the charge front has reached the drain, the entire channel will contain an unbroken sequence of contiguous domains in steady state, the domains forming spontaneously within a few microns of the source. For the conditions in the figure, the domains enter the drain at the rate of 1.38×10^{11} per second, producing an oscillation in the drain current of 138 GHz.

It is a unique feature of our device that the oscillation frequency is determined not by the transit time across the drift channel (v/L), but rather by the transit time across *one period* (λ) of the electron distribution. The computer calculations indicate that the period (λ) is directly proportional to the product $(\bar{n}\mathbf{d})$, where \bar{n} is the average (dc) electron density in the channel, and \mathbf{d} is the separation between the screening electrode and the charge. We can also show that the $(\bar{n}\mathbf{d})$ product must obey

$$\bar{n} \mathbf{d} > \epsilon_s \mathbf{D} / q \mu, \quad (2)$$

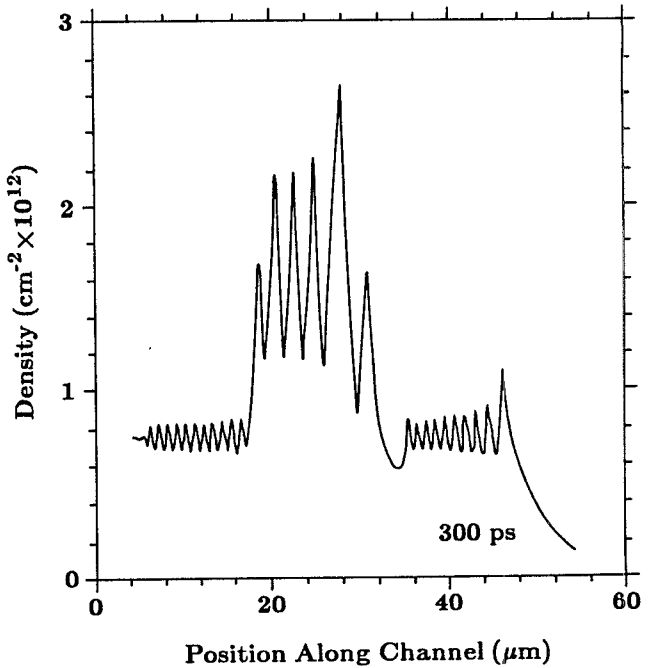


Figure 4. Electron density for the device of Fig. 3, showing the effect of a step change in the injection level. Here, the injection level was initially $7.5 \times 10^{11} \text{ cm}^{-2}$, but was increased to $1.5 \times 10^{12} \text{ cm}^{-2}$ after 100 ps and returned to $7.5 \times 10^{11} \text{ cm}^{-2}$ after 200 ps.

where ϵ_s is the semiconductor permittivity, \mathbf{D} the electron diffusivity at the applied field, q the electronic charge, and μ the magnitude of the (negative) differential mobility at the applied field. Equation (2) bears a striking resemblance to a similar relation for Gunn diodes. A consequence of (2) is that there exists a minimum possible spatial period and thus a maximum possible frequency, limited by the four physical parameters on the right hand side of (2). This limiting frequency is in the range of 200 - 300 GHz.

Because of the dependence of period on the product $(\bar{n}\mathbf{d})$, it is possible to change the frequency of the device by controlling the rate at which electrons are introduced into the channel from the source. This is accomplished by varying the gate-to-source voltage V_{gs} . An example of this control is illustrated in Fig. 4. Here the electron density at the source was held to the value $7.5 \times 10^{11} \text{ cm}^{-2}$ for the first 100 ps of drift, switched to $1.5 \times 10^{12} \text{ cm}^{-2}$ for the next 100 ps, then returned to $7.5 \times 10^{11} \text{ cm}^{-2}$. As seen, the electron density in the channel exhibits a region of high frequency oscillation, followed by a region of low frequency oscillation, followed by a final region of high frequency oscillation. The channel can support regions of different amplitude and period at the same time, since the screening effect of the gate electrode prevents any point in the channel from "seeing" what is going on beyond a distance of about \mathbf{d} away. This figure also illustrates that it is in principle possible to shift the frequency by octaves in a few tens of picoseconds, limited principally by the electronic response time of the gate-to-source circuit.

Computer simulations have been performed for a range of operating conditions, at frequencies extending from 16.5 GHz to 138 GHz. Simulations have not been performed at lower frequencies due to the rapidly increasing

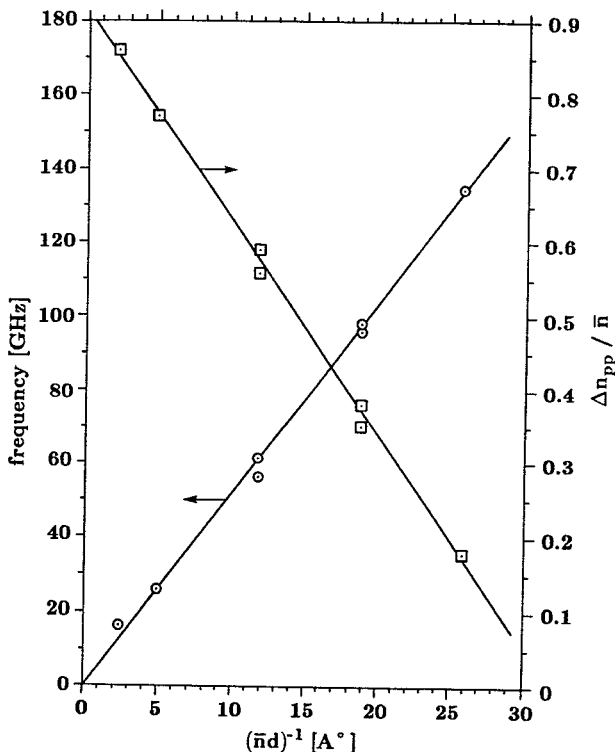


Figure 5. Frequency and normalized peak-to-peak amplitude as a function of the parameter $(\bar{n}d)^{-1}$ for seven different operating conditions. The linearity of these relationships is striking. Note, however, that the actual amplitude (not normalized to \bar{n}) goes as $1/d$ for a given fixed frequency.

ing cost in computer time. However, we expect the lower frequency limit to be determined by the maximum charge capacity of the potential well in the device. It is easy to show that

$$\bar{n} d < 2 \epsilon_s V_{BR} / q, \quad (3)$$

where V_{BR} is the gate voltage which results in semiconductor breakdown. Thus, (2) and (3) effectively determine the operating range of the device. For realistic values of the parameters on the right-hand-sides of (2) and (3), the $(\bar{n}d)^{-1}$ product is confined to the range $0.1 \text{ \AA} \lesssim (\bar{n}d)^{-1} \lesssim 40 \text{ \AA}$. To see how the $(\bar{n}d)^{-1}$ product relates to frequency, we have plotted the results of several simulations in Fig. 5. Here we show frequency and normalized peak-to-peak electron density as a function of $(\bar{n}d)^{-1}$. By reference to Fig. 5, one therefore expects the device to be capable of operation from a few gigahertz to a few hundred gigahertz.

Both the power output and the efficiency can be estimated based on the computer simulations. For example, assuming a 50Ω load, a $500 \mu\text{m}$ wide device with a

channel offset d of 500 \AA would deliver approximately 12 mW at 96 GHz and 0.35 W at 26 GHz . The efficiency at these two frequencies would be about 1.4% and 14% , respectively. (These numbers include about 250 mW in losses due to resistive heating of the gate.) Note that the power output goes as the *square* of w/d , and the efficiency goes up linearly with width w , assuming a fixed drain-to-source voltage. The efficiency of the contiguous-domain device is expected to be relatively high, since the output consists of a continuous ac signal rather than a sequence of isolated pulses (as in the conventional Gunn diode).

The noise figure has not been calculated, but it should be considerably lower than any of the previous microwave oscillators. This is because the contiguous-domain device operates in a steady state rather than a transient fashion, thus reducing noise associated with the charge packet formation process. In fact, it is expected that the noise figure will be comparable with that of the GaAs MESFET, which also operates in steady state.

CONCLUSIONS

We have described a new type of monolithic millimeter-wave oscillator device which makes a clean break from the operating principles of the transit-time limited devices of the past. Our device differs from preceding devices in four fundamental ways: (1) it does not require an external resonant circuit, (2) it employs a two-dimensional electrostatic geometry internally, (3) it does not rely on the transient formation, propagation, and dispersal of pulses of charge, and (4) it is capable of supporting a *contiguous sequence* of charge domains within the drift channel. As a result of these four characteristics, the frequency of our device is not determined by a transit-time effect, but rather by the spatial period of the sequence of charge domains drifting down the channel in steady state. Thus, there is no need for sub-micron drift distances in order to achieve high frequency. Moreover, since there is no external resonant circuit, the frequency can be electrically tuned over a broad bandwidth at high rates. We predict operation in the frequency range from a few gigahertz to a few hundred gigahertz, with the capability of electronically shifting frequency by octaves in a few tens of picoseconds.

REFERENCES

- (1) J. A. Cooper, Jr. and K. K. Thornber, "Screened-Space-Charge, Transferred-Electron Oscillators," *IEEE Electron Device Lett., EDL-6*, 50 (1985).
- (2) S. M. Sze, *Physics of Semiconductor Devices*, 2nd Ed., John Wiley, New York, 1981, p. 424.
- (3) A. M. Mohsen, T. C. McGill, and C. A. Mead, "Charge Transfer in Overlapping Gate Charge-Coupled Devices," *IEEE J. Solid-State Circuits, SC-8*, 191 (1973).